

The Influence of Boundary Conditions to the Electron Properties of Thin Films With Two Sublattices

J.P.Šetrajić, S.M.Stojković, B.S.Tošić

Institute of Physics, Faculty of Sciences, University of Novi Sad,

Trg Dositeja Obradovića 4, 21000 Novi Sad, Yugoslavia

E-mail: bora@unsim.ns.ac.yu; sladja@unsim.ns.ac.yu

I.D.Vragović

Institute of Physics, Technical University Chemnitz, D - 09107, Chemnitz, Germany

E-mail: igor.vragovics@physik.tu-chemnitz.de

D.Popov

University "Politehnica" Timisoara, Piata Horativ 1, 1900 Timisoara, Romania

E-mail: dpopov@edison.et.utt.ro

Abstract

The dispersion law and spectral weights of electrons in perturbed thin film structures with two sublattices was derived by the method of two-time, single-electron Green's functions. In variance from simple cubic structure, electron energy zone splits into two allowed energy bands and forbidden energy gap appears. In contrast to continual energy zone of allowed electron states in bulk crystals, the energy spectra in ultrathin films are discrete. The number of possible energy levels is equal to the double number of film layers along bounded direction. We also analyzed the influence of perturbation energy parameters on electron energy spectra. Increase of the electron energy at the surfaces induces the shift of the spectrum towards higher energies. The width of forbidden energy gap has the greatest value, when electron surface energies are not perturbed. When the transfer energy of electrons at the surfaces increase the spectrum broadens, while width of forbidden gap decreases. The determination of electron space distribution has shown existence of localized states. Through boundary condition variations it is possible to induce appearance of energy gaps inside the spectra (the allowed energy bands of thin film become narrower than those of the bulk) or appearance of localized states (that lie outside bulk limits).

PACS No: 71.10.Fd, 73.20.At, 73.21.Fg, 73.22.Dj

I. INTRODUCTION

Theoretical and experimental studies of quasi-twodimensional crystalline systems (heterostructures, ultrathin films and superlattices) have become rather intense in the last decade [1,2] due to their broader application in nanoelectronics and optoelectronics. The quantum size effects became significant in these structures, which implies essentially different physical properties in comparison to the bulk ones. This is very interesting not only from fundamental physic stand-point, but has great practical importance because electrons are carriers of all transport processes in metals and semiconductors [3,4].

The simplest quantum structures where reduction of dimensionality is applied in only one direction are thin films. After discovering that high temperature superconductive ceramics are layered structure based on alternating CuO_2 planes (with distinct anisotropic physical properties along direction normal to the layers), the interest for thin film was growing [5]. One could reasonably assume that physical properties of thin films contain roots of explanation of high-temperature superconductivity. Therefore, the main part of thin films investigations is devoted to the their superconductive properties. Efforts are mainly focused to stimulated effects with goal to enhance superconductive critical temperature (by suitable electron distribution) [5,6]. In different samples of ceramics, effects important for applications have been investigated [7].

The development of very sophisticated techniques of epitaxial film growth enables the production of high-quality thin-film structures as well as systems film/substrate consisting different combination of materials (metallic/dilectric, metallic/semiconductive, etc.) or systems of alternating thin films, i.e. superlattices¹. This opened up possibilities for novel experimental and theoretical investigations of great variety of physical properties. The electron structure of thin film growing on different substrates studied by means of angle-

¹In some superlattices, for instance, a novel vertical stacking mechanism has been found that gives direct control of the size of the self-organized quantum dots [8].

resolved ultraviolet photoemission spectroscopy (ARPUS) [9]. Direct characterization of occupied quantum well (QW) states² has largely been effected through the use of ARPUS while, k -resolved inverse photoemission spectroscopy has been used in a similar fashion to study unoccupied QW states [10]. The photoemission intensities from the QW states are shown to have a very strong and oscillatory dependence on the photon energy, an effect which could markedly influence the interpretation of QW photoemission studies from rough films at fixed photon energy. Furthermore, electron scattering experiments have been performed for achieving better understanding of the transport properties of thin films as well as transmission probability across film/substrate interface [11].

Considerable interest attracted optical properties of thin films and excitonic effects in these structures [12]. Time resolved photoluminescence (PL) spectroscopy has proved to be a powerful tool for the study of exciton lifetimes and exciton-population relaxation. Theoretical investigations (by Green's function method) [13] of radiative lifetimes of free and localized excitons in QW shown that localized excitons play important role in the PL decay times [13]. A polariton-based theory of resonant Rayleigh scattering in quantum-wells, i.e. the linear elastic scattering of light, near an excitonic resonance have been developed to establish the connection between disorder associated with interface defect and the angular dependence of temporally scattered light under sub- sp resonant excitation of QW. It is found that the spatial correlations between defects scatter a substantial part of the photogenerated excitons to large-wave-vector nonradiative surface-polariton states [14].

In this work we shall numerically analyze electron spectra in infinite as well as in bounded perturbed crystalline structures with complex lattice and compare them with our previous results for ultrathin films with simple cubic lattice [15-17]. Our work shows influence of

²The existence of quantum-well states in thin metal films on metal surface is now well established, and in the case of noble metal/transition metal layers and multilayers, these states have been implicated in the magnetic coupling which can lead to giant magnetoresistance in these films.

boundary conditions to some fundamental physical properties of thin films. We have chosen the Green's functions method [18] which is widely used in quantum solid state theory today for calculation of microscopic as well as macroscopic, equilibrium and nonequilibrium properties of many-particle systems.

II. ELECTRONS IN BULK STRUCTURE

In order to find dispersion law of electrons in thin films with two sublattice (type NaCl) we should, firstly, calculate it for corresponding bulk structure. We shall start analysis of electron subsystem using tight-binding electron Hamiltonian (in nearest-neighbor approximation) in configuration space [3]:

$$H = \sum_{\vec{n}} \Delta_{\vec{n}} a_{\vec{n}}^{\dagger} a_{\vec{n}} - \sum_{\vec{n}, \vec{\lambda}} W_{\vec{n}, \vec{n} + \vec{\lambda}} a_{\vec{n}}^{\dagger} a_{\vec{n} + \vec{\lambda}}. \quad (1)$$

Quantities $a_{\vec{n}}^{\dagger}$ and $a_{\vec{n}}$ are electron creation and annihilation operators on the lattice site \vec{n} . Quantity $\Delta_{\vec{n}}$ denotes the electron energy localized on the site \vec{n} , while $W_{\vec{n}, \vec{n} + \vec{\lambda}}$ are matrix elements of electron transfer (electron jumps) between neighbor sites (\vec{n} and $\vec{n} + \vec{\lambda}$). The properties of electronic subsystem can be analyzed using the single-electron Green's function [18]:

$$G_{\vec{n}; \vec{m}}(t) = \Theta(t) \langle \{ a_{\vec{n}}(t), a_{\vec{m}}^{\dagger}(0) \} \rangle_0 \quad (2)$$

and solving its standard equation of motion [15-18]. Performing the standard procedure and time Fourier transformation [15-17], we obtain:

$$\hbar\omega G_{\vec{n}; \vec{m}}(\omega) = \frac{i\hbar}{2\pi} \delta_{\vec{n}; \vec{m}} \Delta_{\vec{n}} G_{\vec{n}; \vec{m}}(\omega) - \sum_{\vec{\lambda}} W_{\vec{n}, \vec{n} + \vec{\lambda}} G_{\vec{n} + \vec{\lambda}; \vec{m}}(\omega). \quad (3)$$

This equation, because of its general character, can be used for the analysis of ideal infinite structures as well as of structures with broken translational symmetry. In crystals with two sublattice we introduce the following quantities: $\Delta_{\vec{n}} \rightarrow \Delta^a$ and $\Delta_{\vec{n} + \vec{\lambda}} \rightarrow \Delta^b$. The equation for Green's functions splits into two equations. After total space Fourier transformation one obtains:

$$\hbar\omega G^a = \frac{i\hbar}{2\pi} + \Delta^a G^a - 2(W_x \cos a_x k_x + W_y \cos a_y k_y + W_z \cos a_z k_z)G^b \quad (4)$$

$$\hbar\omega G^b = \frac{i\hbar}{2\pi} + \Delta^b G^b - 2(W_x \cos a_x k_x + W_y \cos a_y k_y + W_z \cos a_z k_z)G^a . \quad (5)$$

One can get the electron dispersion law for bulk system, calculating the Green's function poles in (ω, \vec{k}) space (which define the spectrum of possible electron energies). The solutions of the system of equations of motion can be expressed as ratio of the corresponding variable determinant and the system determinant, i.e. $G = \frac{D_G}{D}$. The determination of Green's function poles turns into the calculation of the roots of the system determinant, i.e. condition $D = 0$.

Evaluating the system determinant (where $E = \hbar\omega$), introducing new parameter $\theta = \Delta^b/\Delta^a$, the electron dispersion law becomes:

$$E = (1 + \theta) \frac{\Delta^a}{2} \pm \frac{1}{2} \sqrt{[(1 - \theta)\Delta^a]^2 + 16 \left(\sum_{i=x,y,z} W_i \cos a_i k_i \right)^2} . \quad (6)$$

Fig.1

The electron energy spectra in bulk crystal with complex lattice (for $k_x = k_y = 0$, $\Delta^a = 6W_z$ and $\theta = 0.5$) is depicted in Fig.1. The continual bulk energy zone splits into two bands of allowed electron states, separated by the forbidden energy gap. Characteristic reduced energies ($\mathcal{E} \equiv \frac{\hbar\omega}{W}$) for bulk system were calculated from equation (6), putting $k_x = k_y = 0$ and $k_z = 0$ for \mathcal{E}_{l_m} and \mathcal{E}_{h_M} , and $k_z = \pi$ for \mathcal{E}_{l_M} and \mathcal{E}_{h_m} and they are

$$\mathcal{E}_{l_m} = -1.68 ; \mathcal{E}_{l_M} = 2.00 ; \mathcal{E}_{h_m} = 7.00 ; \mathcal{E}_{h_M} = 10.68 , \quad (7)$$

where $\mathcal{E}_{(l/h)_m}$ minimal and $\mathcal{E}_{(l/h)_M}$ maximal reduced energies of lower (l) and higher (h) energy bands. It is obvious that forbidden energy band is: $\mathcal{E}_f = \mathcal{E}_{h_m} - \mathcal{E}_{l_M} = 5.00$.

On this level we complete the electron Green's function theory of unbounded structures necessary for applying to electron system with broken translational symmetry and for comparison for their corresponding physical quantities.

III. ELECTRON ENERGY SPECTRA IN FILM STRUCTURES

Real crystals, in difference to ideal infinity structures, do not have property of translational invariance. The existence of certain boundary conditions introduce translational symmetry breaking, which can be introduced by index n_z , because in XY planes, the film is infinite, but in z direction it has a finite thickness (L). Index n_z can takes values $n_z = 0, 1, 2, \dots, N_z$; where $N_z \in [2, 20]$.

We consider that crystalline film is made on (100) substrate which can be of different material than the film. Other boundary surface can be in contact with vacuum, for instance, or with the same material as substrate is³. Due to presence of the inter-atom interactions (between film and surrounding medium) in the boundary layers, electron energies ($\Delta^{a/b}$) and hopping terms (W) values are changed, which is taken into account by introducing boundary conditions, i.e. perturbation parameters: parameters $\varepsilon_{0/N_z}^{a/b}$ describe the relative change of electron energy ($\Delta^{a/b}$) on the surface layers ($n_z = 0$, and $n_z = N_z$), while $w_{0/N_z}^{a/b}$ describe the relative change of electron transfer W_z between surface layers and their adjacent. Because of that, in Hamiltonian (1) we introduce the following boundary conditions:

$$\begin{aligned}
 W_{n_z, n_z-1} &\equiv W_z^{a/b} = W_z (1 + w_0^{a/b} \delta_{1, n_z}^{b/a} + w_{N_z}^{b/a} \delta_{N_z, n_z}^{b/a}) \\
 W_{n_z, n_z+1} &\equiv W_z^{a/b} = W_z (1 + w_0^{a/b} \delta_{0, n_z}^{a/b} + w_{N_z}^{b/a} \delta_{N_z-1, n_z}^{a/b}) \\
 \Delta_z^{a/b} &= \Delta^{a/b} (1 + \varepsilon_0^{a/b} \delta_{0, n_z}^{a/b} + \varepsilon_{N_z}^{b/a} \delta_{N_z, n_z}^{b/a})
 \end{aligned} \tag{8}$$

Because of the system confinement, only partial space Fourier transformation (along x and y directions) can be performed [15-17]. After that, we obtain two sets of non-homogeneous algebraic-difference equations for $2(N_z + 1)$ Green's functions. The first set:

³It is so called sandwiched film. Sandwiches of differently doped films have been used as model system to study the magnetic field induced metal-to-insulator transition in quantum wells (see e.g. [10] and references therein).

$(G_0^a, G_1^b, G_2^a, \dots, G_{N_z-1}^a, G_{N_z}^b)$ corresponds to atomic line (along z direction) with atom "a" at the first XY -layer ($n_z = 0$), while the second set: $(G_0^b, G_1^a, G_2^b, \dots, G_{N_z-1}^b, G_{N_z}^a)$ corresponds to atomic line with atom "b" at the first layer. $G_{n_z}^{a/b} = 0$ for the $N_z < n_z < 0$. The first set of equations has the following general form:

$$\begin{aligned}
\hbar\omega G_{2j;m_z}^a &= \frac{i\hbar}{2\pi} \delta_{2j;m_z}^a + \Delta^a (1 + \varepsilon_0^a \delta_{0,n_z}^a) G_{2j;m_z}^a - W_z G_{2j-1;m_z}^b - \\
&\quad - W_z (1 + w_0^a \delta_{0,n_z}^a + w_{N_z}^b \delta_{N_z-1,n_z}^a) G_{2j+1;m_z}^b - \\
&\quad - 2G_{2j;m_z}^b (W_x \cos a_x k_x + W_y \cos a_y k_y) \\
\hbar\omega G_{2j+1;m_z}^b &= \frac{i\hbar}{2\pi} \delta_{2j+1;m_z}^b + \Delta^b (1 + \varepsilon_{N_z}^b \delta_{N_z,n_z}^b) G_{2j+1;m_z}^b - \\
&\quad - W_z (1 + w_0^a \delta_{1,n_z}^b + w_{N_z}^b \delta_{N_z,n_z}^b) G_{2j;m_z}^a - W_z G_{2j+2;m_z}^a - \\
&\quad - 2G_{2j+1;m_z}^a (W_x \cos a_x k_x + W_y \cos a_y k_y)
\end{aligned} \tag{9}$$

The second set of equations is equivalent to the first (it must be replaced $a \leftrightarrow b$). The general form of the second set is then:

$$\begin{aligned}
\hbar\omega G_{2j;m_z}^b &= \frac{i\hbar}{2\pi} \delta_{2j;m_z}^b + \Delta^b (1 + \varepsilon_0^b \delta_{0,n_z}^b) G_{2j;m_z}^b - \\
&\quad - W_z G_{2j-1;m_z}^a - W_z (1 + w_0^b \delta_{0,n_z}^b + w_{N_z}^a \delta_{N_z-1,n_z}^b) G_{2j+1;m_z}^a - \\
&\quad - 2G_{2j;m_z}^a (W_x \cos a_x k_x + W_y \cos a_y k_y) \\
\hbar\omega G_{2j+1;m_z}^a &= \frac{i\hbar}{2\pi} \delta_{2j+1;m_z}^a + \Delta^a (1 + \varepsilon_{N_z}^a \delta_{N_z,n_z}^a) G_{2j+1;m_z}^a - \\
&\quad - W_z (1 + w_0^b \delta_{1,n_z}^a + w_{N_z}^a \delta_{N_z,n_z}^a) G_{2j;m_z}^b - W_z G_{2j+2;m_z}^b - \\
&\quad - 2G_{2j+1;m_z}^b (W_x \cos a_x k_x + W_y \cos a_y k_y)
\end{aligned} \tag{10}$$

where following shortnotes were introduced:

$$\varrho = \frac{\hbar w}{W_z} - \frac{\Delta^a}{W_z}; \quad R = 2 \frac{W_x \cos a_x k_x + W_y \cos a_y k_y}{W_z} \tag{11}$$

$$\mathcal{K}_{n_z;m_z}^{a/b} = \frac{i\hbar}{2\pi} \frac{\delta_{n_z;m_z}^{a/b}}{W_z}; \quad \theta = \frac{\Delta^b}{\Delta^a}$$

In order to perform the basic task of this research, determination of electron energies, we must calculate Green's function poles [18]. The determination of Green's functions poles

turn into the calculation of the roots of the determinant D of the system formed by sets (9) and (10), i.e. solving the condition $D = 0$. In the general case, the condition $D = 0$ is not analytically solvable, so numerical methods must be applied. As an example, we study the case $\theta = 0.5$, i.e. $\Delta_b = 0.5\Delta_a$, $W_x = W_y = W_z \equiv W$ for various film widths ($N_z + 1 \in [3, 13]$). We use that perturbation parameters the same surface should be similar to each other: $w_0^a \approx w_0^b \equiv w_0$; $w_{N_z}^a \approx w_{N_z}^b \equiv w_{N_z}$ and $\varepsilon_0^a = \varepsilon_0^b \equiv \varepsilon_0$; $\varepsilon_{N_z}^a = \varepsilon_{N_z}^b \equiv \varepsilon_{N_z}$.

Results derived by numerical methods are presented in Figs.2,3,4 and Table 1. Particularly, we analyzed the influence of boundaries and film thickness as well as influence of perturbation parameters to the electron spectra.

Due to existence of spatial confinement, energy spectra of electrons in thin film with complex lattice is discrete (as in the case of film with simple lattice [15-17]). Number of possible energy levels is equal to the double number of film layers along finite direction, as depicted in Fig.2, for perturbation parameters: $\varepsilon_{0/N_z} = w_{0/N_z} = 0$ [19]. In this case we are dealing with ideal surfaces (model of ideal thin film which has been "cut-off" from an identical infinity structure), and these boundary conditions are known as Dirichlet boundary conditions [15-17,19,20]. One can see that discrete energy zone splits into two allowed energy bands and forbidden gap appears. In contrast to allowed energy bands in bulk crystal, energy bands in film are narrower, so the energy gaps appear [15]. Thus, consequence of the spectrum discreteness is the existence of minimal non-zero energy, i.e. of the bottom energy gap.

Fig.2

Minimal (\mathcal{E}_{l/h_m}) and maximal (\mathcal{E}_{l/h_M}) reduced energies of lower (l) and higher (h) energy bands and the width of forbidden gap (\mathcal{E}_f) strongly depend on film thickness [20]. The bottom and the top energy gaps decreases with the increasing of film width (as in the case of film with simple lattice [15-17]). The forbidden gap width is greater for ultrathin films, while it decreases towards the bulk value for thick films.

Electron energy spectra depends on values of perturbation parameters, as in simple thin films [16,17]. Increase of electron energy at boundary surfaces (parameters ε) induces the shift of the spectrum towards higher energies (the increase of the bottom gap and decrease of the top gap), while for the increase of the electron energy transfer inside surface layers (parameters w), the spectrum broadens (the decrease of both bottom and top gap).

Depending on values of the parameters of surface interaction, certain energy levels can lie outside allowed energy bands, even in forbidden energy zone, so localized states of electrons appear [16,20]. As an example, for the parameters $w_0 = 0.6; w_{N_z} = -0.6; \varepsilon_0 = 0.5$ and $\varepsilon_{N_z} = -0.5$, four localized states appear (two in forbidden energy gap ($\mathcal{E}_{3/4}$), one below bottom energy gap (\mathcal{E}_1) and one above top energy gap (\mathcal{E}_4)). The energy of these states depends on film width, which is shown on Table 1. By increasing film thickness the energies of localized states alienate from characteristic bulk values, scaling to one constant value. On this way, forbidden gap becoming of constant width, lower than in the bulk.

Table 1

For certain values of parameters there are two localized states, both above the maximal or minimal bulk energy. Energies of these states depend on film thickness. For the greater film width, these two states become one, as shown in Fig.3 for top localized states and corresponding⁴ states in forbidden zone, for parameters: $w_0 = w_{N_z} = 1, \varepsilon_0 = \varepsilon_{N_z} = 0.5$.

Fig.3

The width of the forbidden energy zone depend on the values of the perturbation energy parameters, which is shown on Fig.4 ($\varepsilon_0 = \varepsilon_{N_z} = \varepsilon$ and $w_0 = w_{N_z} = w$). When the

⁴It is shown that with appearance of top/bottom localized states simultaneously appear states in lower/higher part of forbidden zone.

perturbation parameters of electrons transfer energy decrease, the width of forbidden energy gap increase. If film does not have perturbation (on surface layers along z direction) on electron energy localized on surface layers ($\varepsilon = 0$), than the forbidden energy gap would have the maximal value, as it is depicted on Fig.4.

Fig.4

The applied one-particle approximation is reasonable if this model of film is taken as weak semiconductor. The quasi-particle method has been shown to be very accurate and capable of predicting the excitation for a variety of systems (metals, semiconductors, bulk, surfaces, etc.). For a system of alternating semiconductive thin films, consisting two different kind of atoms, such as GaN or AlN, this method [21] has given good agreement with experiments. It has been shown that in these weak semiconductors energy zone splits into two allowed bands, as in our model [12]. For one-particle states interaction with transverse electromagnetic field gives rise to interband and intraband transitions (which are made possible by discretization of the energy levels of thin film [12]), while for two-particle states gives rise to polariton effects. Obtained dispersion law of electrons in thin films can be probed experimentally by process of polariton scattering on one electron [12-14], since energies of polaritons and electrons are the same order of magnitude [22].

The mixed group of alloys such as those composed GaN and GaAs or AlN and AlAs should, in principle, allow us to close the gap between the nitrides and arsenides, making possible the fabrication of III-V light emitting devices covering complete spectrum (see e.g. [21] and references therein). We have shown, in this paper, that by changing of boundary conditions one can affects forbidden zone width and, consequently, optical properties of thin films [12,23].

IV. SPECTRAL WEIGHTS AND SPACE DISTRIBUTION

Space distribution of electrons can be found determining Green's functions and after that calculating spectral weights of given electron state for each film layer. The starting point is the system of equations for Green's functions (9) and (10), written in matrix form.

$$\hat{\mathcal{D}}\tilde{\mathcal{G}} = \tilde{\mathcal{K}}, \quad (12)$$

where $\hat{\mathcal{D}}$ is $2(N_z + 1)$ order system matrix, while $\tilde{\mathcal{G}}$ and $\tilde{\mathcal{K}}$ are Green's functions and delta vectors:

$$\tilde{\mathcal{G}} = \begin{pmatrix} G_{0,m_z} \\ G_{1,m_z} \\ \cdot \\ \cdot \\ G_{n_z,m_z} \\ \cdot \\ \cdot \\ G_{N_z,m_z} \end{pmatrix}, \quad \tilde{\mathcal{K}} = \frac{i\hbar}{2\pi W_z} \begin{pmatrix} \delta_{0,m_z} \\ \delta_{1,m_z} \\ \cdot \\ \cdot \\ \delta_{n_z,m_z} \\ \cdot \\ \cdot \\ \delta_{N_z,m_z} \end{pmatrix}.$$

Applying inverse matrix $\hat{\mathcal{D}}^{-1}$ we get: $\tilde{\mathcal{G}} = \hat{\mathcal{D}}^{-1}\tilde{\mathcal{K}}$. We calculated only diagonal Green's functions $G_{n_z;n_z}$, because of their importance in equilibrium processes. Factorizing multipole functions we obtain [24]:

$$G_{n_z;n_z} = \frac{i\hbar}{2\pi V_z} \sum_{\nu=1}^{N_z+1} \frac{g_{n_z;n_z}(\varrho_\nu)}{\varrho - \varrho_\nu}. \quad (13)$$

Spectral weights $g_{n_z;n_z}(\varrho_\nu)$ are given by:

$$g_{n_z;n_z} = \frac{D_{n_z;n_z}(\varrho_\nu)}{\frac{d}{d\varrho}D(\varrho)|_{\varrho=\varrho(\nu)}} \quad (14)$$

and satisfy the sum rules: $\sum_{n_z=0}^{2N_z} g_{n_z;n_z}(\varrho_\nu) = 1$ and $\sum_{\nu=1}^{2(N_z+1)} g_{n_z;n_z}(\varrho_\nu) = 1$.

Spectral weights, representing the squared moduli of wave functions, enable us to analyze space distribution of electrons along z direction. Beside, when the diagonal component of

Green's function matrix are known, one can compute the local densities of the electron states and Fermi energy (as is shown for model of simple film [17]).

That is depicted on Fig.5a,b for various thickness of films $N_z + 1 \in \{3, 4\}$ of ideal (unperturbed) film [19].

Fig.5

In case of ideal film (Dirichlet boundary conditions) only bulk states can appear, which can be interpreted as quantum-well states. Space distributions (for both atomic lines along z -directions) are symmetrical because of crystal symmetry. By increasing film thickness, the spectral weights of states with lowest and highest energies decrease.

Fig.6

In case of perturbed film space distribution is influenced by perturbation parameters values, which is shown on Fig.6. For states that lie outside bulk limits, probability of finding an electron in certain position is the maximal in the boundary layers with a sharp decrease in inside layers, therefore these states are localized electron states [20]. Space distribution is symmetrical (as in unperturbed film) if electron energy at surface is same as bulk ones and all states are bulk. In all other cases symmetry is disturbed and one atomic line is "favored" (spectral weights are higher than in other atomic line), which is shown in Fig.6a : $\varepsilon_{0/N_z} = -0.5$; $w_{0/N_z} = 0.5$ and Fig.6b: $\varepsilon_{0/N_z} = 0.5$; $w_{0/N_z} = 0.5$.

V. CONCLUSION

In this paper the Green's function method is applied in order to calculate electron dispersion law and spectral weights of thin film with two sublattices. The analysis of electron properties of thin films has indicated a large influence of boundary conditions.

1. In contrast to the continual energy zone of allowed electron states in bulk crystals, the electron energy spectra in ultrathin films are discrete. The number of possible energy levels is equal to the double number of film layers along bounded direction. The consequence of the spectrum discreteness is the existence of the bottom (minimal non-zero energy) and the top energy gaps, which decrease with the increasing of the film width. The energy zone of possible electron states in films is narrower than in the bulk.
2. In variance from single-atom structures, continual electron energy zone splits into two allowed energy bands and forbidden energy gap appears. The width of the forbidden gap is greater for ultrathin films and decreases with the increasing of the number of film layers, coinciding with the bulk value for $N_z \rightarrow \infty$. The width of forbidden energy gap has the greatest value, when electron surface energies are not perturbed.
3. By suitable choice of perturbation energy parameters, quantum well and/or localized states appear. Number and position of these states are determined by number of layers in crystalline system and values of perturbation parameters. This influences forbidden gap width and consequently optical properties of film.

The described model and given microtheoretical approach open a possibility to study various physical properties and phenomena of thin films. Green's function method applied here, enables the consistent derivation of some statistical values and properties of the thin film (thermodynamic, transport and dielectric, which have been successfully calculated for thin film with simple lattice [23-25]).

The interest to described structures in material science is based on the possibility of manipulation of the physical properties of materials and devices by changing of characteristic parameters. The most important of those properties are superconductivity (connected to existence, distribution and width of energy gaps [5,6]), optical properties (connected to distribution of localized states and width of forbidden gap [12-14,23]), surface effect [16,20], transport characteristic [4] and similar phenomena.

REFERENCES

- [1] Nanostructure Physics and Fabrication, edited by M. A. REED and W. P. KIRK, Academic, Boston, 1989.
- [2] M. G. COTTAM and D. R. TILLEY, Introduction to Surface and Superlattice Excitations, Univ.Press, Cambridge, 1989.
- [3] G. MAHAN, Many Particle Physics, Plenum Press, New York, 1990.
- [4] C. W. J. BEENAKKER and H. VAN HOUTEN, Quantum Transport in Semiconductor Nanostructures, Sol.Stat.Phys. Vol. 44: Semiconductor Heterostructures and Nanostructures, Academic, Boston, 1991.
- [5] L. L. CHANG and L. ESAKI, Phys.Today, Oct.36 (1992).
- [6] S. F. YOON, Y. B. MIAO and K. RADHAKISNAN, Thin Solid Films **279**, 11 (1996).
- [7] Y. SATO and D. SATO, Thin Solid Films **281-282**, 445 (1996).
- [8] L. WANG, P. KRATZER and M. SCHEFFLER, Jpn.J.Appl.Phys. **39**, 4298 (2000).
- [9] M. MILUN, P. PERVAN, B. GUMHALTER and D. P. WOODRUFF, Phys.Rev. B **59**, 5170 (1999).
- [10] D. P. WOODRUFF, M. MILUN and P. PERVAN, J.Phys.Con.Matt. **11**, 105 (1999).
- [11] J. E. ORTEGA, F. J. GARCIA DE ABAJO, P. M. ECHENIQUE, I. MANKE, T. KALKA, M. DAHNE, D. OCHS, S. L. MOLODOTSOV and A. RUBIO, Phys.Rev. B **58**, 2233 (1998).
- [12] L.C.ANDREANI, Confined Electrons and Photons: Optical Transitions, Excitons and Polaritons in Bulk and Low-Dimensional Semiconductive Structures, ed. by E.Burstein and C.Weisbuch, Plenum Press, New York, 1995.
- [13] D. S. CITRIN, Phys.Rev. B **47**, 3832 (1993).

- [14] D. S. CITRIN, Phys.Rev. B **54**, 14 572 (1996).
- [15] D. LJ. MIRJANIĆ, J. P. ŠETRAJČIĆ, S. M. STOJKOVIĆ, I. D. VRAGOVIĆ and S. K. JAĆIMOVSKI, IEEE - Proc. on 21st International Conference on Microelectronics **1**, 121 (1997).
- [16] J. P. ŠETRAJČIĆ, S. M. STOJKOVIĆ, B. ABRAMOVIĆ and S. LAZAREV, Bal.Phys.Lett. **5**, 414 (1997).
- [17] S. B. LAZAREV, M. PANTIĆ and B. S. TOŠIĆ, Physica A **246**, 53 (1997).
- [18] G. RICKAYZEN, Green's Functions and Condensed Matter, Academic Press, London, 1980.
- [19] I. D. VRAGOVIĆ, S. M. STOJKOVIĆ, J. P. ŠETRAJČIĆ, D. ŠIJAČIĆ, I. JUNGER, D. LJ. MIRJANIĆ and S. M. VUČENOVIĆ, Bul.Stii.Univ. Politehnica Timisoara (Mat.Fiz.) **45**, 70 (2000).
- [20] S. G. DAVISON and M. STESLICKA, Basic Theory of Surface States, Clarendon, Oxford, 1996.
- [21] A. RUBIO and M. L. COHEN, Phys.Rev. B **51**, 4343 (1995).
- [22] V. M. AGRANOVICH and O. A. DUBOVSKI, Effect of Retarded Interaction of the Exciton Spectrum in One-Dimensional and Two-Dimensional Crystals, JETP Lett. **3**, 223 (1966).
- [23] J. P. ŠETRAJČIĆ, D. LJ. MIRJANIĆ, V. D. SAJFERT, B. S. TOŠIĆ and R. P. DJAJIĆ, Physica A **190**, 363 (1992).
- [24] B. S. TOŠIĆ, M. PANTIĆ and S. B. LAZAREV, J.Phys.Chem.Solids **58**, 1995 (1997).
- [25] S. B. LAZAREV, M. R. PANTIĆ, S. M. STOJKOVIĆ, B. S. TOŠIĆ and J. P. ŠETRAJČIĆ, J.Phys.Chem.Solids **61**, 931 (2000).

TABLES

N_z	\mathcal{E}_1	\mathcal{E}_2	\mathcal{E}_3	\mathcal{E}_4
3	-2.018	2.653	6.176	11.810
4	-2.032	2.693	6.166	11.845
5	-2.035	2.698	6.164	11.849
6	-2.036	2.699	6.164	11.8496
7	-2.036	2.699	6.164	11.8496
8	-2.036	2.699	6.164	11.8497
9	-2.036	2.699	6.164	11.8497
10	-2.036	2.699	6.164	11.8497
11	-2.036	2.699	6.164	11.8497
12	-2.036	2.699	6.164	11.8497
13	-2.036	2.699	6.164	11.8497

TABLE I. Localized electron states

FIGURES

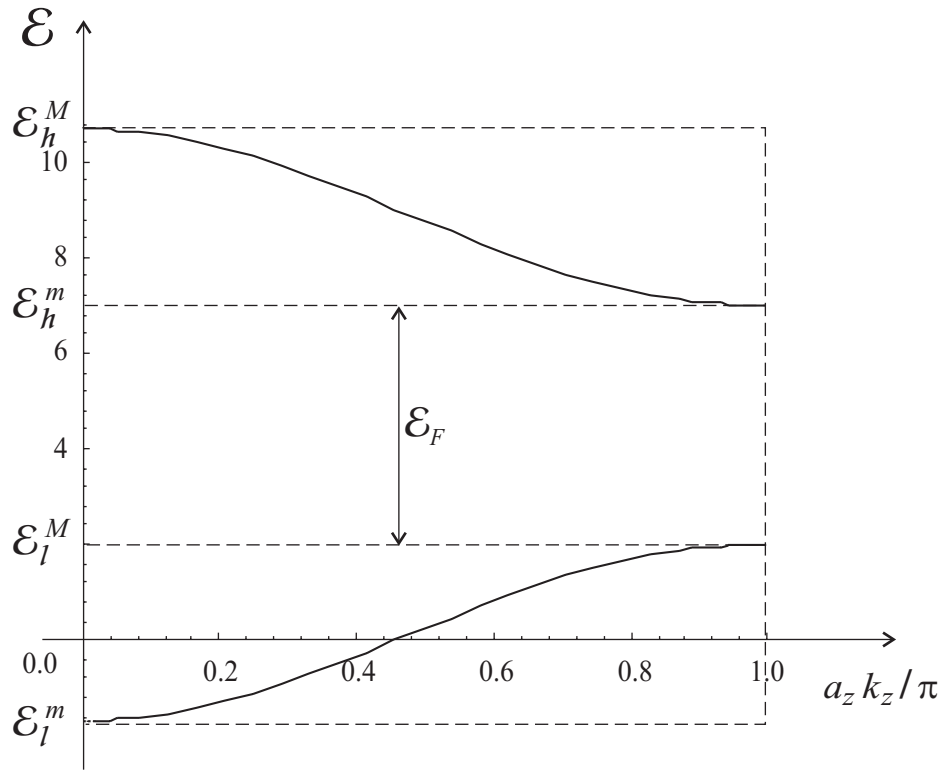


FIG. 1. The electron energy spectra in bulk crystal

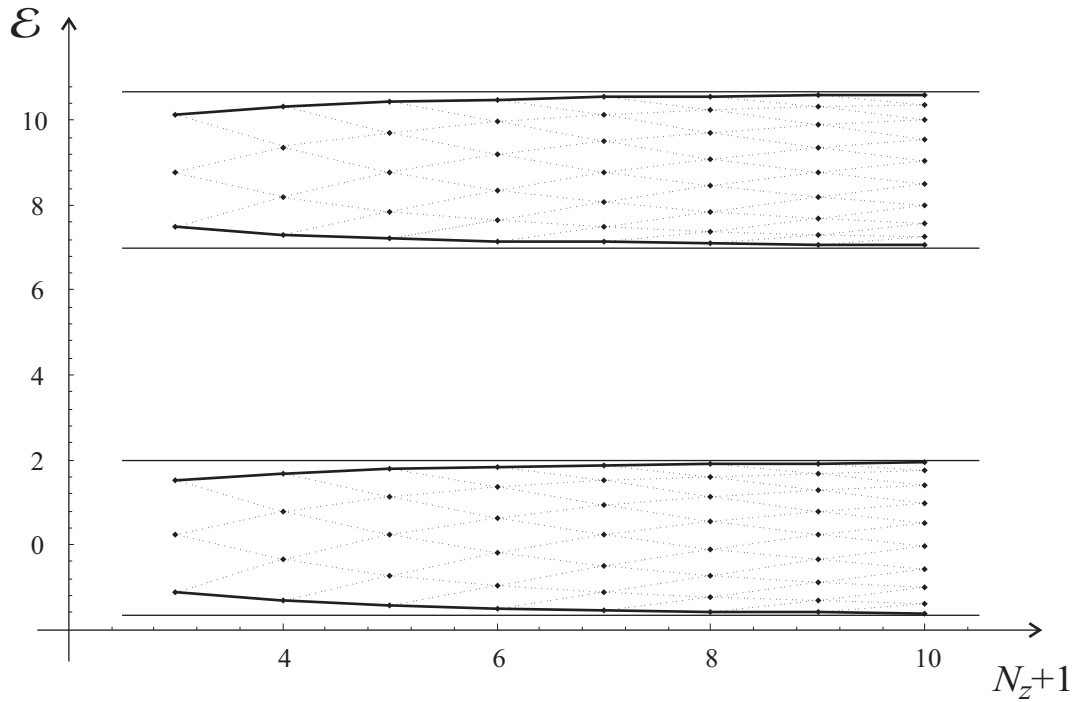


FIG. 2. The electron energy spectra dependence on film thickness

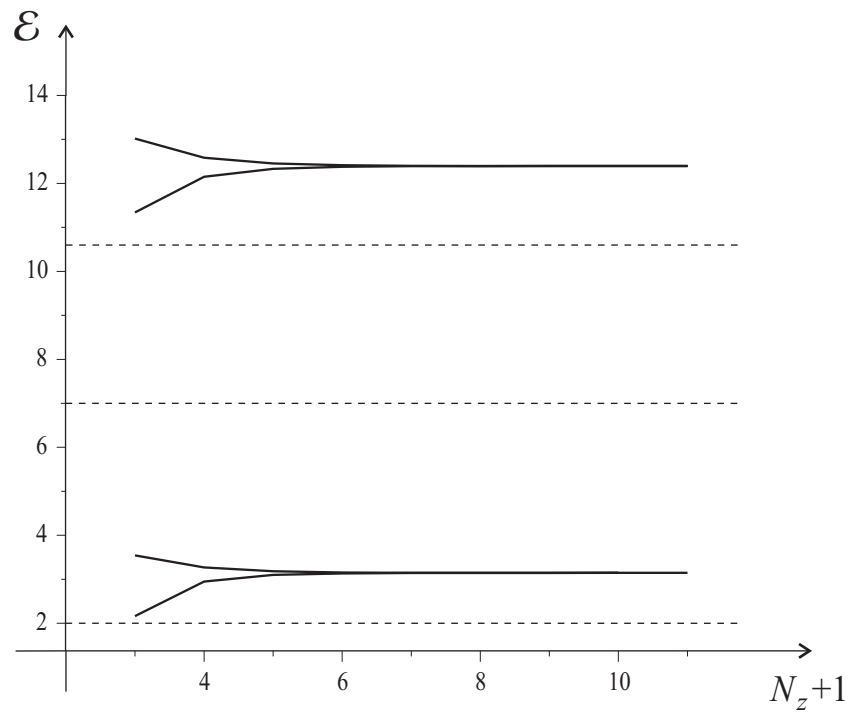


FIG. 3. Localized electron states

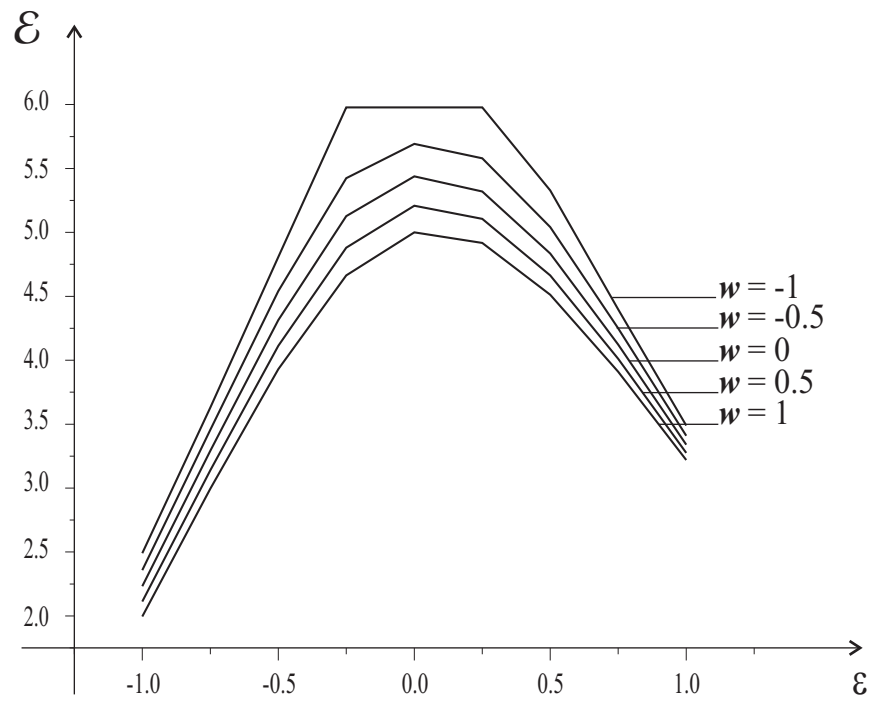


FIG. 4. Width of forbidden zone dependence on boundary conditions

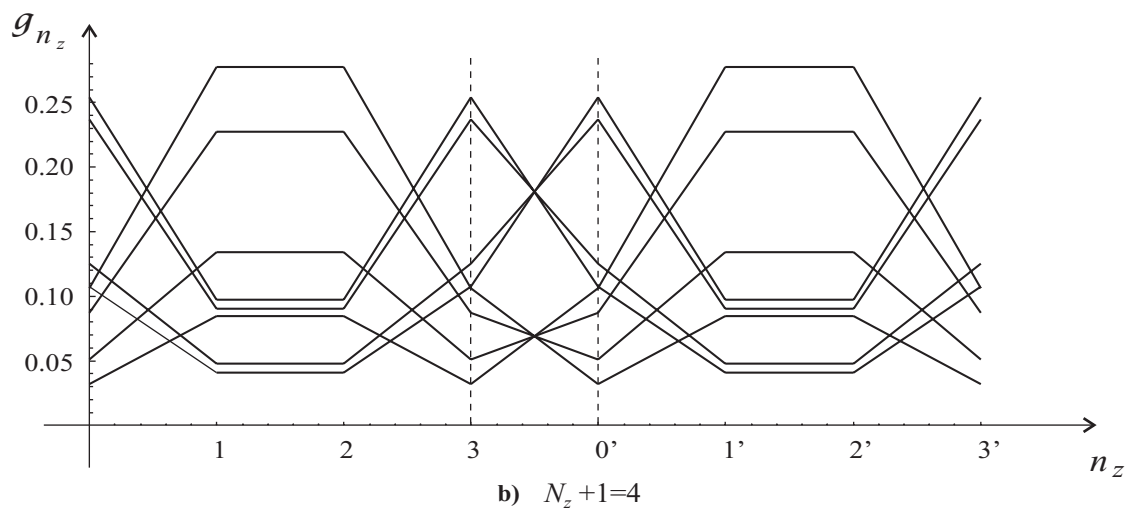
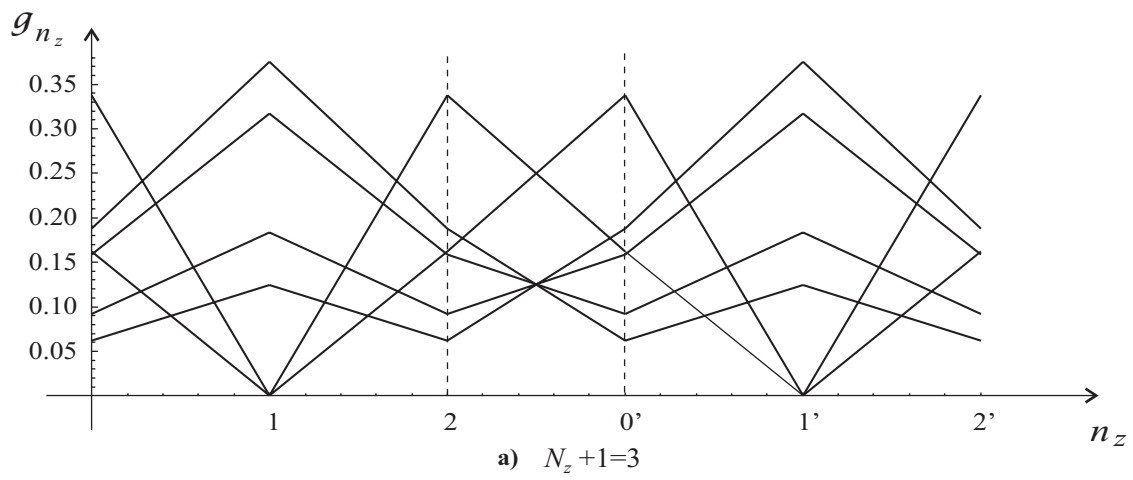


FIG. 5. Spectral weights of unperturbed film

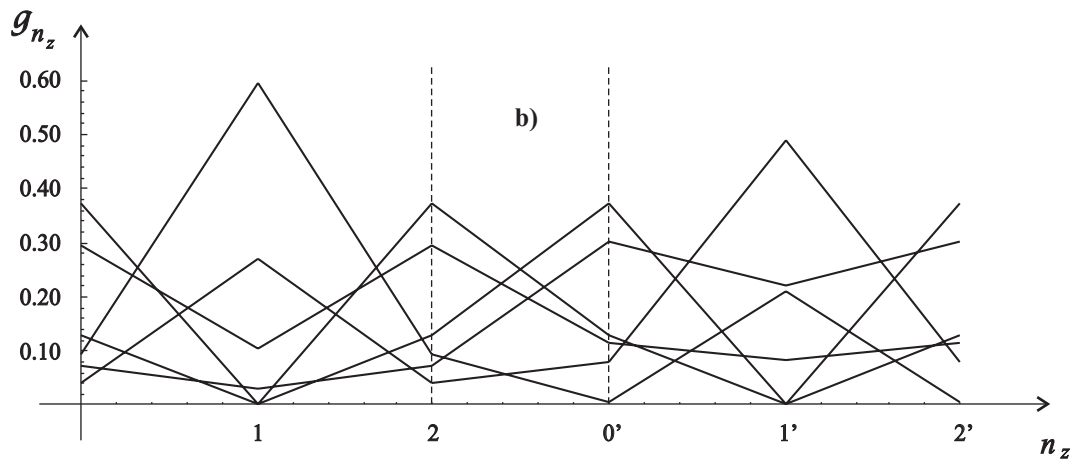
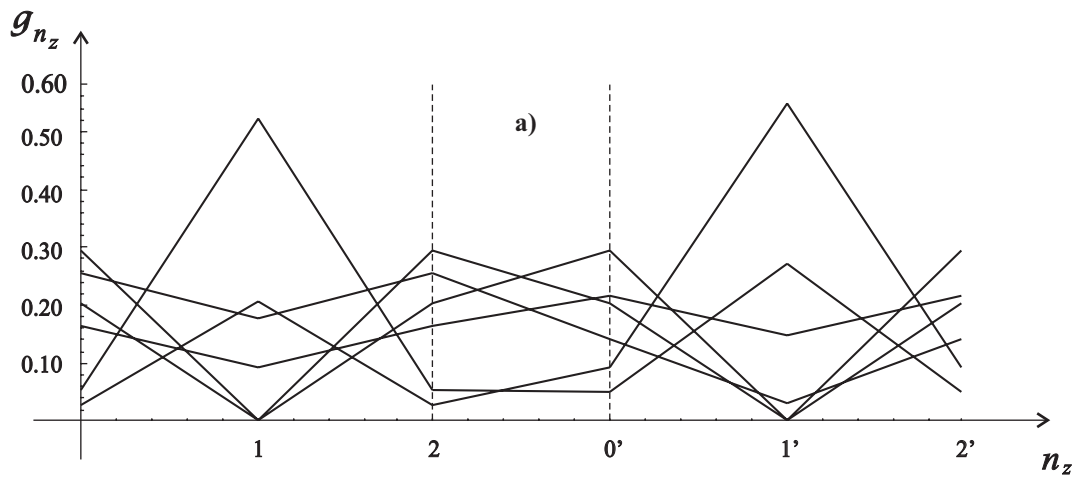


FIG. 6. Spectral weights of perturbed film